ACS Catalysis

pubs.acs.org/acscatalysis
Letter

Iron-Catalyzed *Ipso*-Nitration of Aryl Borides via Visible-Light-Induced β-Homolysis

Shuyang Liu, Yusheng Lu, Hongyao Wang, Zhiyan Xue, Ziyi Xu, Huihui Wan, Qingxin Yin, Tianming Lv, Shu-Xin Liu,* and Yunhe Jin*

Cite This: *ACS Catal.* 2025, 15, 3306−3313
Read Online

ACCESS | Metrics & More | Article Recommendations | Supporting Information

ABSTRACT: Herein, we reported a practical method to realize *ipso*-nitration of boronic acids, their pinacol esters, and trifluoroborate salts with alkali metal salt $NaNO_3$ as a nitrating reagent. A Fe^{III}/Fe^{IV} catalytic cycle involving an unusual visible-light-induced β-homolysis pathway of the N−O bond in a simple iron complex effectively provides a nitryl radical as the key nitrating species. This protocol bears mild reaction conditions, a broad scope (up to 99% yield), good functional group compatibility, and convenient scale-up synthesis.

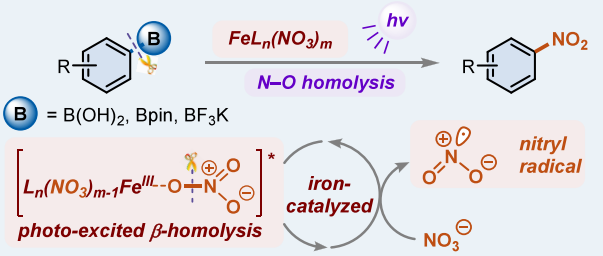

KEYWORDS: *Photocatalysis, Iron catalysis, Nitryl radical, Aryl boride, β-homolysis*

INTRODUCTION

Nitroaromatic compounds play a vital role in synthetic organic chemistry because of their easy transformation to amides, azenes, amines, and heterocycles.[1] They have been widely employed in a variety of fields, such as pharmaceuticals,[2] agriculture,[2c,d] materials,[3] dyes,[4] and explosives.[1] As one of the most extensively researched organic reactions, the build of nitroaromatic compounds always depends on a well-known process called the "mixed acid" approach in which nitronium ions (NO_2^+) as nitrating species are produced by combining nitric acid with concentrated sulfuric.[1,5] Although this process is still utilized in industries, the downsides are clear. As a typically notoriously polluting process, the superstoichiometric usage of acids and the unavoidable generation of nitrogen oxide (NO_x) fumes and wasted acids result in poor functional group tolerance as well as difficulty in separating the desired products.[6] To address these issues, new strategies were carried out in the past few decades.[7] Among them, *ipso*-nitration has emerged as an efficient method as it effectively circumvents the regioselectivity issue.[8] Aryl boronic acids and their derivatives, as easily synthesized and commercial chemicals, have been widely used as starting materials to produce aromatic compounds with diverse functional groups.[1a,9] In past decades, various approaches for the *ipso*-nitration of aryl boronic acids have been reported.[10] Some early year impressive methods go through mechanisms based on the nitronium ion, while overchemometric strong acids and high temperatures are always necessary (Scheme 1a).[10a−d] Many pioneering works were developed for achieving *ipso*-nitration of aryl boronic acids in recent years with the nitryl radical generated from superstoichiometric *tert*-butyl nitrite or $Bi(NO_3)_3/NaNO_2$ with strong oxidants (Scheme 1b).[10d−h] Furthermore, novel organic nitrating reagents have also been discovered, bringing milder conditions for *ipso*-nitration as well as complex processes for preparing them.[10d,g] Therefore, gentle, efficient, and environmentally friendly protocols for accessing *ipso*-nitration with the most low-cost nitrate $NaNO_3$ remain to be developed.

In the past decade, photocatalysis has been developed as an environmentally friendly, sustainable, and unique process for organic transformations.[11] High-activity radicals generated by photoactive complexes with earth-abundant metals play an important role in a wide range of reactions under mild conditions.[12] Recently, an emerging mode of photoactivation has taken the spotlight, based on an inner-sphere mode of reactivity triggered by a population of ligand-to-metal charge-transfer (LMCT) excited states. LMCT excitations tend to promote homolysis of the metal−ligand bond, resulting in the formation of the reduced metal complex and ligand-centered radicals. Numerous simple complexes of earth-abundant transition metals were reported to be able to perform this distinctive photoinduced α-homolysis process by many other distinguished groups[13] including us.[13i−l] Very recently, our group reported an enzyme-mimicking protocol on visible-light-driven arene C−H nitration with stoichiometric ferric nitrates as the nitrating reagent.[14] Through an unusual β-homolysis of a ferric nitrate complex, a nitryl radical is generated and proven

Received: November 25, 2024
Revised: February 4, 2025
Accepted: February 4, 2025

Scheme 1. Approaches for *ipso*-Nitration of Aryl Boronic Acids

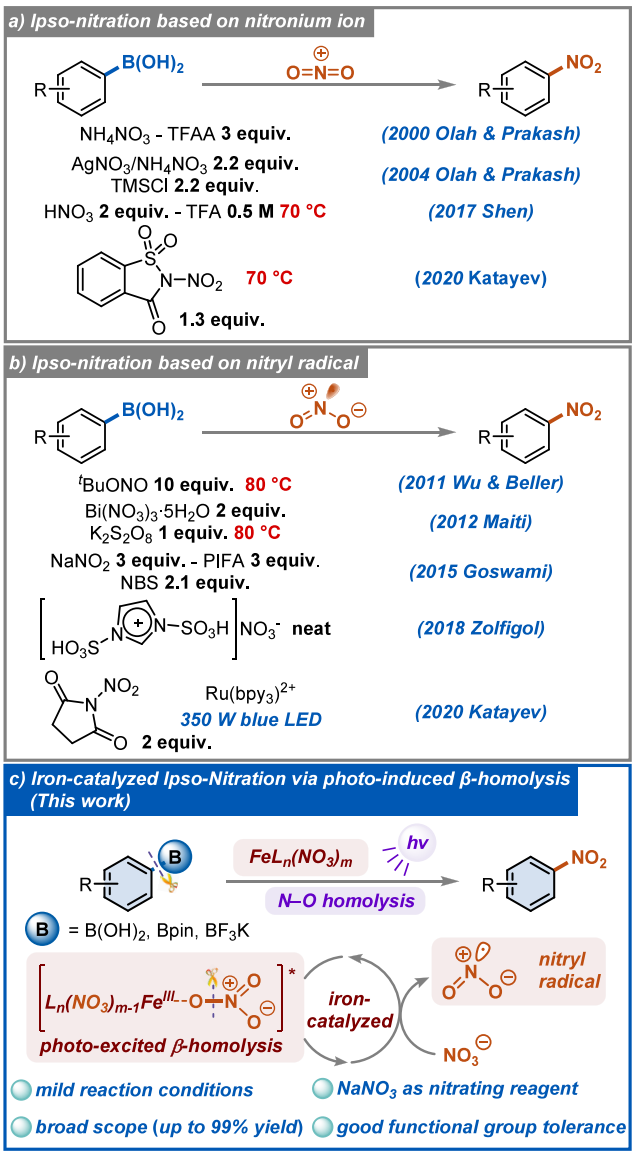

to be the key nitrification species. In light of these observations, we hypothesize that this pathway can be applied in *ipso*-nitration reactions, bringing operational convenience and environmental benefit. Meanwhile, the high activity of borides may improve this system from a stoichiometric protocol to a catalytic pathway. Herein, we successfully present the iron-catalyzed approach for visible-light-induced *ipso*-nitration of aryl borides with alkali metal salt $NaNO_3$ as the nitrating reagent (Scheme 1c). A broad scope of aryl boronic acids, their pinacol esters, and trifluoroborate salts were efficiently *ipso*-nitrated via catalytic β-homolysis under mild conditions.

RESULTS AND DISCUSSION

We started our exploration with the model reaction using 4-biphenylboronic acid (**12a**) in the presence of $Fe(NO_3)_3 \cdot 9H_2O$ (10 mol %) and $NaNO_3$ (1.0 equiv) in MeCN under irradiation of 395 nm LEDs at room temperature for 8 h (Table 1, entry 1). Fortunately, 4-nitrobiphenyl (**12b**) was detected by GC-MS with a large amount of starting materials

Table 1. Optimization of the Reaction Conditions[a]

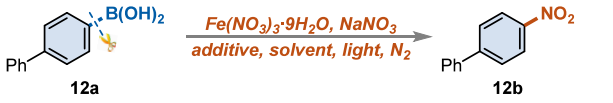

12a 12b

entry	additive	solvent	light	yield [%][b]
1		MeCN	395 nm	trace
2[c]	HNO_3	MeCN	395 nm	6
3	TFA	MeCN	395 nm	12
4	HF	MeCN	395 nm	17
5	HBF_4	MeCN	395 nm	50
6	HPF_6	MeCN	395 nm	28
7	HBF_4	MeCN	365 nm	trace
8	HBF_4	MeCN	405 nm	59
9	HBF_4	MeCN	427 nm	68
10	HBF_4	MeCN	455 nm	90 (88[d])
11	HBF_4	MeCN	CFL	30
12	HBF_4	MeCN	sunlight	35
13	HBF_4	acetone	455 nm	22
14	HBF_4	DCM	455 nm	N.R.
15	HBF_4	THF	455 nm	trace
16	HBF_4	DMSO	455 nm	N.R.
17[e]	HBF_4	MeCN	455 nm	54
18[f]	HBF_4	MeCN	455 nm	65
19[g]	HBF_4	MeCN	455 nm	N.R.
20	HBF_4	MeCN		N.R.

[a]Reaction conditions: **12a**, 0.2 mmol, $Fe(NO_3)_3 \cdot 9H_2O$ 10 mol %, $NaNO_3$ 1.0 equiv, additive 1.5 equiv, solvent 2 mL, 30 W LED, N_2, rt, 8 h. [b]^{1}H NMR yield. [c]0.5 equiv of HNO_3 and $NaNO_3$ was added. [d]Isolated yields. [e]Under O_2. [f]Under air. [g]No $Fe(NO_3)_3 \cdot 9H_2O$.

remaining. Investigation of additives revealed that acids were able to boost the yield to varying extents (entries 2−6), and we assume that the addition of acids can help neutralize the resulting alkaline ferric complex and complete the catalytic cycle. Among them, acids containing fluorine were found to be effective (entries 4−6), and HBF_4 appeared to be the best choice (entry 5). This might be because the fluoride ions can accelerate the exit process of boron. Then, different illumination wavelengths were tried to promote the reaction efficiency. We were pleased to find as the illumination wavelength of the LEDs increased, the yield of **12b** had a steady-state growth (entries 7−10) and reached its highest point of 90% at 455 nm (entry 10). Switching the visible light source from 455 nm to CFL (compact fluorescent lamp) or sunlight resulted in lower yields (entries 11, 12). Later, the effect of solvents was also investigated, and other solvents, such as acetone, DCM, THF, and DMSO afforded lower yields of **12b** than MeCN (entries 13−16). Variations in atmospheres exhibited no positive effects (entries 17, 18). Control experiments indicated that the reaction did not occur without iron as the catalyst or visible light as an energy source (entries 19, 20).

With the optimized reaction conditions in hand, various arylboronic acids were first subjected to examination of the generality of our protocol. As depicted in Scheme 2, a broad range of electron-rich arylboronic acids performed well, affording the corresponding nitroaromatics in moderate to excellent yields (**1b**−**34b**). Different alkyl (**2b**−**7b**) and ether-substituted (**14b**, **15b**) arylboronic acids were all suitable substrates and could deliver corresponding *ipso*-nitration products in good to excellent yields. As vital synthons, halogen substituents (**8b**−**10b**), as well as bromomethyl (**11b**),

https://doi.org/10.1021/acscatal.4c07252
ACS Catal. 2025, 15, 3306−3313

Scheme 2. Substrate Scope for the Visible-Light-Induced *ipso*-Nitration of Aryl Boronic Acids[a,b]

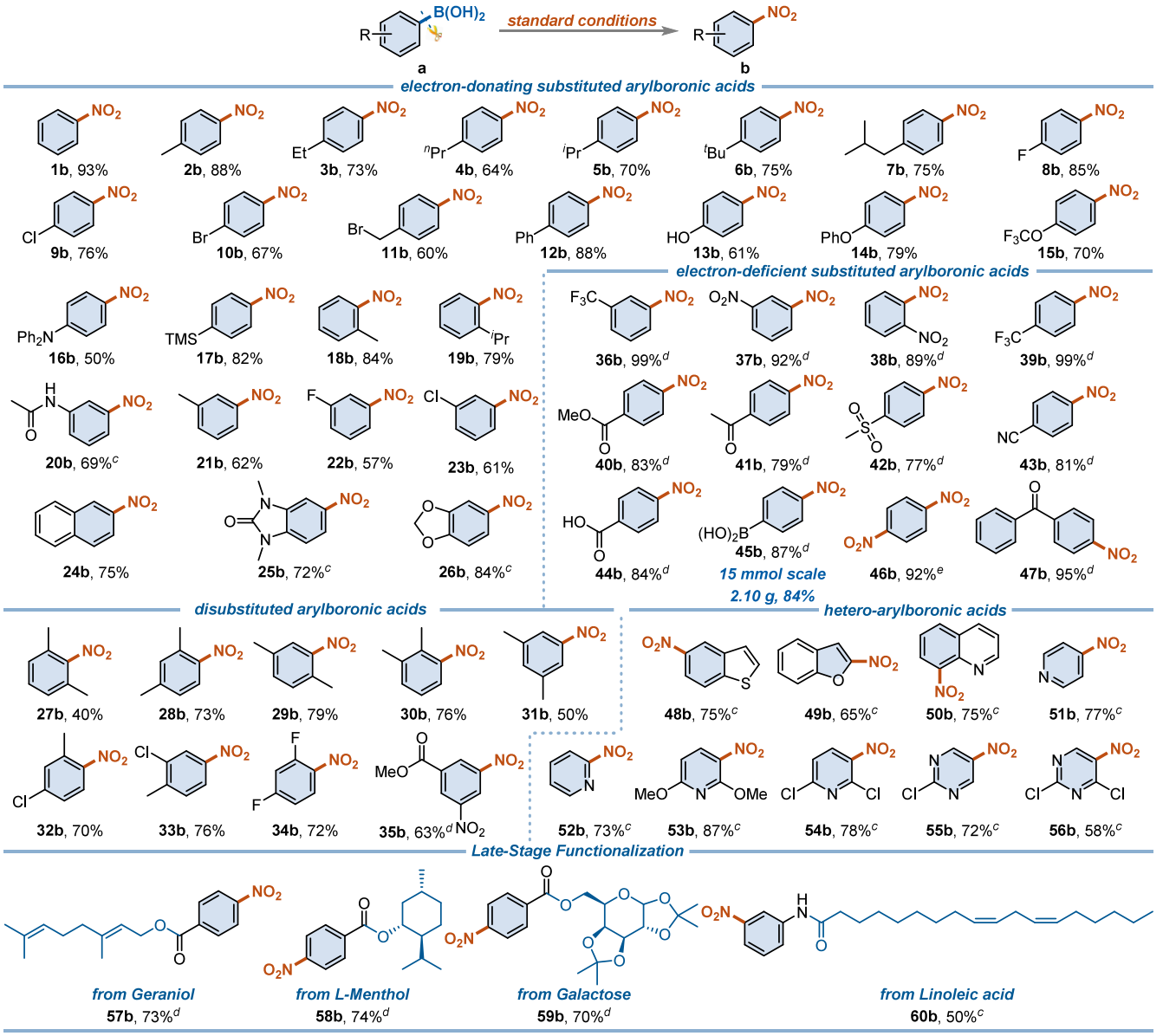

[a]Reaction conditions: Aryl boronic acid a, 0.2 mmol, $Fe(NO_3)_3{\cdot}9H_2O$ 10 mol %, $NaNO_3$ 1.0 equiv, HBF_4 1.5 equiv, MeCN 2 mL, 30 W 455 nm LED, N_2, rt, 8 h. [b]Isolated yield. [c]1.5 equiv of HPF_6 was used instead of HBF_4. [d]1.5 equiv of $NaNO_3$ and 3.0 equiv of HBF_4 were added. [e]Three equiv of $NaNO_3$ and 6.0 equiv of HBF_4 were added.

performed well and gave the corresponding *ipso*-nitration products in good yields, leaving ample room for further cross-couplings. Active groups, including hydroxyl (**13b**) and trimethylsilyl (**17b**), also remained untouched, offering a good chance for further derivatization. As a vital core structure in electroactive and photoactive materials,[15] triarylamine was involved in the substrate (**16b**), and the reaction performed well. Aniline derivatives (**20b**) also supplied the desired product in a good yield, providing the potential for late-stage functionalization of natural products. Boronic acids with naphthalene, benzoimidazole, and benzodioxole rings were employed next, and the corresponding products were achieved in satisfactory yields (**24b**−**26b**). Arylboronic acids with *ortho* and *meta* substituents were also viable substrates, affording exclusively mononitrated arenes in medium to good yields (**18b**−**23b**). Disubstituted arylboronic acids also supplied the *ipso*-nitration product in satisfactory yields (**27b**−**35b**). *Ortho*-disubstituted arylboronic acid gave a relatively low yield, probably due to the steric effects. Notably, after proper adjustments of the reaction conditions, we were gratified to find that a variety of electron-deficient substituents also participated in the reaction well. Substrates with trifluoromethyl (**36b**, **39b**), nitro (**37b**, **38b**), ester (**40b**), ketocarbonyl (**41b**, **47b**), sulfonyl (**42b**), cyano (**43b**), carboxyl (**44b**), and arylboronic acid (**45b**) were all readily converted to the corresponding *ipso*-nitration products efficiently. The substituent position showed little effect on the reaction with the corresponding products, both obtained in excellent yields (**36b** and **39b**; **37b** and **38b**). Furthermore, mono- or dinitration could be conveniently modulated for 1,4-phenylenediboronic acid by the usage of different equivalences of sodium nitrate and acid (**45b** and **46b**), offering a good

https://doi.org/10.1021/acscatal.4c07252
ACS Catal. 2025, 15, 3306−3313

Scheme 3. Substrate Scope for the Visible-Light-Induced *ipso*-Nitration of Other Aryl Borides[a,b]

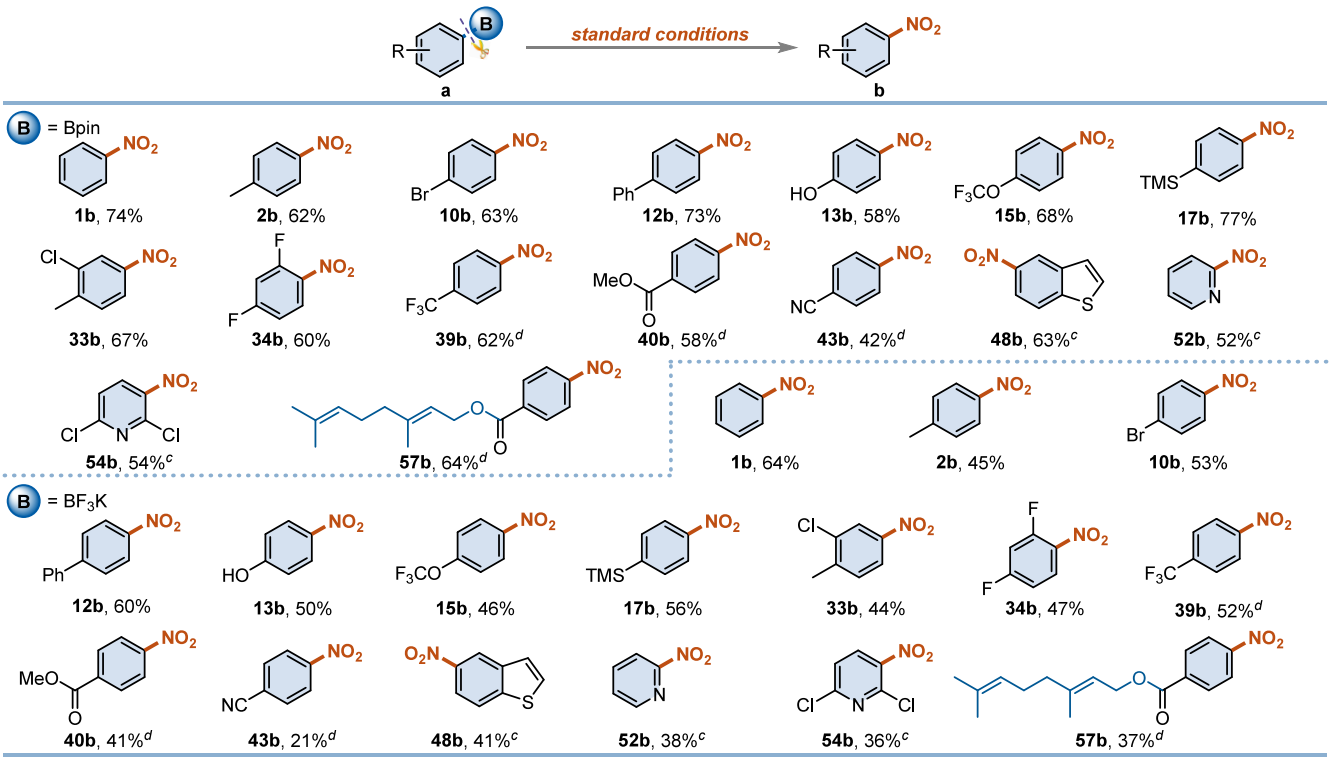

[a]Reaction conditions: Aryl borides a, 0.2 mmol, $Fe(NO_3)_3{\cdot}9H_2O$ 10 mol %, $NaNO_3$ 1.0 equiv, HBF_4 1.5 equiv, MeCN 2 mL, 30 W blue LED, N_2, rt, 16 h. [b]^{1}H NMR yield, 1, 3, 5-trimethoxybenzene as the internal standard. [c]1.5 equiv of HPF_6 was used instead of HBF_4. [d]1.5 equiv of $NaNO_3$ and 3.0 equiv of HBF_4 was added.

Scheme 4. Mechanistic Studies

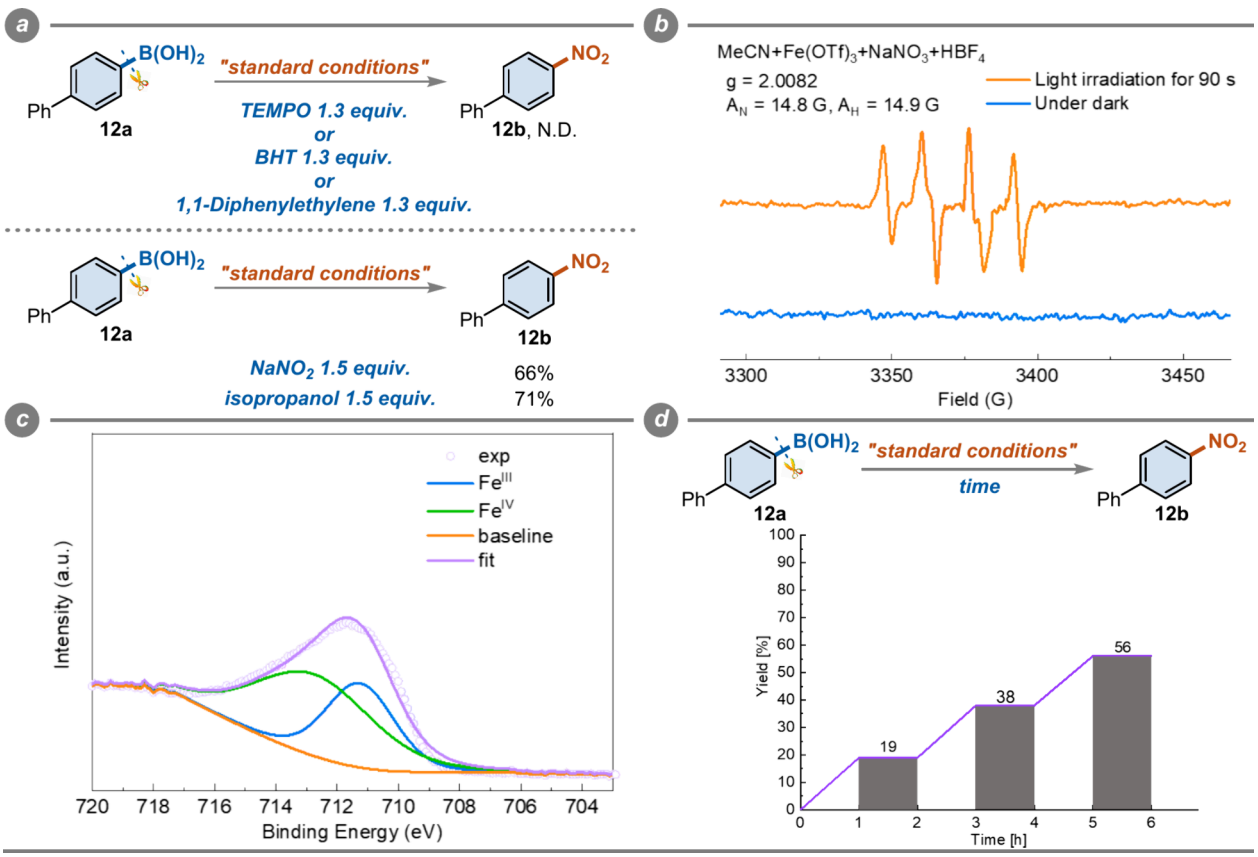

https://doi.org/10.1021/acscatal.4c07252
ACS Catal. 2025, 15, 3306−3313

Scheme 5. Proposed Mechanism

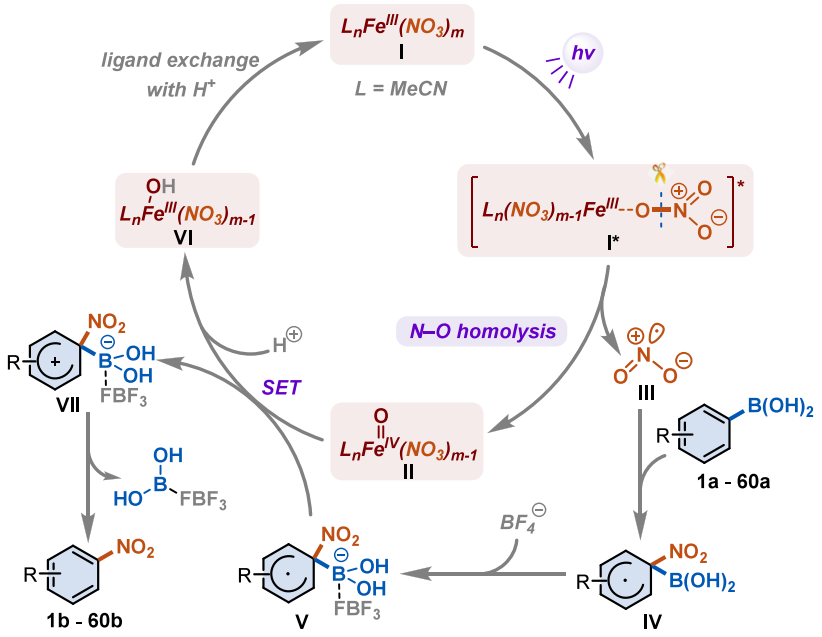

chance for further cross-couplings. A dielectron-withdrawing-group substituted for aryl boronic acid offered the desired product in a moderate yield (**35b**). To further illustrate the practicability of this method, a gram-scale reaction was performed, producing 2.10 g of **45b** in 84% yield without the obvious loss of efficiency (see details in the SI, part IV). In addition, we were pleased to find that a wide range of heteroarylboronic acids were also suitable substrates. Various nitrated heteroaryl rings such as thianaphthene (**48b**), benzofuran (**49b**), quinoline (**50b**), pyridines (**51b**−**54b**), and pyrimidines (**55b**, **56b**) were obtained in medium to good yields through this method.

Expanding the applicable scope to late-stage photonitration of biorelevant compounds will greatly enhance the application value of our strategy in functional molecule modification. For this purpose, substrates with types of biogenic complex molecules were tried, and the corresponding products from olefin (**57b**), terpene (**58b**), carbohydrate (**59b**), and fatty acid (**60b**) were all achieved in gratifying yields, further demonstrating the good active group tolerance, certain biocompatibility, and great potential in the postmodification of complex molecules for this protocol.

Furthermore, we investigated the utilization of our protocol with different aryl boride substrates (Scheme 3). It was demonstrated that boronic acid pinacol ester and trifluoroborate salt substrates were both effective candidates in the reaction, although the reaction efficiency was slightly lower than that for the corresponding boronic acids (**1b**, **2b**, **10b**, **12b**, **13b**, **15b**, **17b**, **33b**, **34b**, **39b**, **40b**, **43b**, **48b**, **52b**, **54b**, and **57b**). After prolonging the reaction time, the nitration yields for boronic acid pinacol esters could almost reach the ones for boronic acids. By contrast, only moderate to good results were obtained for trifluoroborate salts due to their poor solubility in acetonitrile. Both electron-rich and electron-deficient boronic acid pinacol ester and trifluoroborate salt substrates can produce corresponding desired nitro arene product smoothly, and active groups including halogen (**10b**, **33b**, **34b**), hydroxyl (**13b**) and trimethylsilyl (**17b**) still remained untouched, providing a good chance for further derivatizations. Disubstituted aryl borides (**33b**, **34b**) and aryl borides containing biogenic skeletons (**57b**) are all suitable substrates, providing good chances for further utilization in late-stage functionalization. Heteroarylboronic acid pinacol ester and trifluoroborate salt substrates can also be converted to the corresponding *ipso*-nitration products efficiently (**48b**, **52b**, **54b**).

To probe in detail the reaction mechanism, several trapping experiments were conducted first. When stoichiometric 2,2,6,6-tetramethylpiperidinooxy (TEMPO), 2,6-di-*tert*-butyl-4-methylphenol (BHT), and 1,1-diphenyl-ethylene were respectively added to the reaction system, the yields of **12b** were slashed dramatically, which suggested that a radical process should be involved (Scheme 4a). In addition, stoichiometric OH radical scavengers ($NaNO_2$ and isopropanol) were, respectively, added to the reaction system. The outcomes showed the yields of **12b** reduced slightly, suggesting that the OH radical might make a little contribution to this system (Scheme 4a). Furthermore, electron spin resonance (ESR) experiments were performed to distinguish the radical category. The ESR spectrum of a mixture of $Fe(OTf)_3$, HBF_4, and $NaNO_3$ in MeCN with 5,5-dimethyl-1-pyrroline *N*-oxide (DMPO) as a radical spin trap under dark conditions showed no signal of a trapped radical. After irradiation for 90 s, an obvious quartet signal (g = 2.0082, A_N = 14.8 G, A_H = 14.9 G) was observed, indicating the appearance of a nitryl radical[16] (Scheme 4b). To further determine the valence state change of iron after the generation of a nitryl radical, X-ray photoelectron spectroscopy (XPS) detection was carried out. As shown in Scheme 4c, the peaks located at 711.30 and 713.10 eV in the Fe $2p_{3/2}$ XPS spectra of the iron residue were respectively attributed to Fe^{III} and Fe^{IV} according to the reported literature,[17] indicating that the system undergoes an Fe^{III}−Fe^{IV} pathway instead of the Fe^{III}−Fe^{II} pathway in the traditional LMCT system. The competition reaction of **12a** and **34a** showed the reactivity of the reaction was affected by electronic effects (see details in the SI, part III, iv). Similar outcomes were also acquired when

https://doi.org/10.1021/acscatal.4c07252
ACS Catal. 2025, 15, 3306−3313

analyzing the substrate scope. A light-on−off experiment was carried out next, revealing that continuous light irradiation was crucial for this transformation (Scheme 4d).

Based on the above results and our reported literature,[14] a plausible reaction mechanism for the present visible-light-induced iron-catalyzed *ipso*-nitration of aryl borides was proposed in Scheme 5. Initially, photoactive complex **I** composed of a ferric ion center and several nitrate/acetonitrile ligands was stimulated to reach excited state **I*** under light irradiation. A spontaneous β-N−O homolysis released desired nitryl radical **III** and Fe^{IV}=O complex **II**. A subsequent electrophilic addition between electron-deficient radical **III** and aryl boronic acid **a** resulted in cyclic radical **IV**. Later, with the stabilization of the tetrafluoroborate ion, a SET occurred between intermediate **V** and Fe^{IV}=O complex **II**, generating cation intermediate **VII** and protonated iron complex **VI**. The subsequent deboronation of intermediate **VII** produced the desired product. Finally, an *in situ* neutralization and ligand exchange of complex **VI** regenerated photoactive complex **I**.

CONCLUSION

In summary, we have developed an effective system for visible-light-driven iron-catalyzed aryl boride *ipso*-nitration under mild conditions. The reaction shows high efficiency, broad scope, good functional group tolerance, a cheap and safe nitration reagent, and some potential in complex molecule modification and late-stage functionalization. The reaction could be easily scaled up and controlled by different equivalences of nitrates. Moreover, it is expected that the present nitryl radical generation via photocatalytic β-homolysis will help inspire chemists to uncover other novel strategies for nitration chemistry.

MATERIALS AND METHODS

All information regarding the materials and methods used in this study is reported in the Supporting Information.

ASSOCIATED CONTENT

Supporting Information

The Supporting Information is available free of charge at https://pubs.acs.org/doi/10.1021/acscatal.4c07252.

Mechanism investigations, synthetic procedures, characterization data, and NMR spectra of these synthesized compounds (PDF)

AUTHOR INFORMATION

Corresponding Authors

Shu-Xin Liu − *Department of Nephrology, Dalian Municipal Central Hospital affiliated with Dalian University of Technology, Dalian Key Laboratory of Intelligent Blood Purification, Dalian 116033, China*; Email: shuxinliu@dlut.edu.cn

Yunhe Jin − *State Key Laboratory of Fine Chemicals, School of Chemistry, Dalian University of Technology, Dalian 116024, China*; orcid.org/0000-0003-0626-4587; Email: jinyh18@dlut.edu.cn

Authors

Shuyang Liu − *State Key Laboratory of Fine Chemicals, School of Chemistry, Dalian University of Technology, Dalian 116024, China; Department of Nephrology, Dalian Municipal Central Hospital affiliated with Dalian University of Technology, Dalian Key Laboratory of Intelligent Blood Purification, Dalian 116033, China*; orcid.org/0009-0001-8246-4970

Yusheng Lu − *State Key Laboratory of Fine Chemicals, School of Chemistry, Dalian University of Technology, Dalian 116024, China*

Hongyao Wang − *State Key Laboratory of Fine Chemicals, School of Chemistry, Dalian University of Technology, Dalian 116024, China*

Zhiyan Xue − *State Key Laboratory of Fine Chemicals, School of Chemistry, Dalian University of Technology, Dalian 116024, China*

Ziyi Xu − *State Key Laboratory of Fine Chemicals, School of Chemistry, Dalian University of Technology, Dalian 116024, China*

Huihui Wan − *Instrumental Analysis Center, Dalian University of Technology, Dalian 116024, China*

Qingxin Yin − *Instrumental Analysis Center, Dalian University of Technology, Dalian 116024, China*

Tianming Lv − *Instrumental Analysis Center, Dalian University of Technology, Dalian 116024, China*

Complete contact information is available at: https://pubs.acs.org/10.1021/acscatal.4c07252

Author Contributions

All authors have given approval to the final version of the manuscript.

Notes

The authors declare no competing financial interest.

ACKNOWLEDGMENTS

We acknowledge the support of the National Natural Science Foundation of China (21901032), the Fundamental Research Funds for the Central Universities (DUT21LK13), and the Applied Basic Research Project of Liaoning Province, China (2023JH2/101300091).

REFERENCES

(1) (a) Clayden, J.; Greeves, N.; Warren, S. *Organic Chemistry*; Oxford University Press, USA, 2012. (b) Ono, N. *The Nitro Group in Organic Synthesis*; John Wiley & Sons, 2003.

(2) (a) Belciug, M.-P.; Ananthanarayanan, V. S. Interaction of calcium channel antagonists with calcium: structural studies on nicardipine and its Ca^{2+} complex. *J. Med. Chem.* **1994**, *37*, 4392−4399. (b) Squella, J.; Bollo, S.; Núñez-Vergara, L. Recent developments in the electrochemistry of some nitro compounds of biological significance. *Curr. Org. Chem.* **2005**, *9*, 565−581. (c) Ju, K.-S.; Parales, R. E. Nitroaromatic Compounds, from Synthesis to Biodegradation. *Microbiol. Mol. Biol. Rev.* **2010**, *74*, 250−272. (d) Nepali, K.; Lee, H.-Y.; Liou, J.-P. Nitro-Group-Containing Drugs. *J. Med. Chem.* **2019**, *62*, 2851−2893.

(3) (a) Fiedler, H.; Mucke, W. Nitro Derivatives of Polycyclic Aromatic Hydrocarbons (NO_2-PAT). *Anthropogenic Compounds* **1991**, *3*, 97−137. (b) Fan, F.-R. F.; Yao, Y.; Cai, L.; Cheng, L.; Tour, J. M.; Bard, A. J. Structure-Dependent Charge Transport and Storage in Self-Assembled Monolayers of Compounds of Interest in Molecular Electronics: Effects of Tip Material, Headgroup, and Surface Concentration. *J. Am. Chem. Soc.* **2004**, *126*, 4035−4042. (c) Liu, M. H.; Liu, C. W. Comparative simulation study of chemical synthesis of functional DADNE material. *J. Mol. Model.* **2017**, *23*, 4.

(4) Langhals, H. Color Chemistry. Synthesis, Properties and Applications of Organic Dyes and Pigments. 3rd revised edition. By Heinrich Zollinger. *Angew. Chem., Int. Ed.* **2004**, *43*, 5291−5292.

(5) Hughes, E. D.; Ingold, C. K.; Reed, R. I. Kinetics of Aromatic Nitration: the Nitronium Ion. *Nature* **1946**, *158*, 448−449.
(6) Olah, G. A.; Narang, S. C.; Olah, J. A.; Lammertsma, K. Recent aspects of nitration: New preparative methods and mechanistic studies (A Review). *Proc. Natl. Acad. Sci. U. S. A.* **1982**, *79*, 4487−4494.
(7) (a) Yan, G.; Yang, M. Recent advances in the synthesis of aromatic nitro compounds. *Org. Biomol. Chem.* **2013**, *11*, 2554−2566. (b) Song, L.-R.; Fan, Z.; Zhang, A. Recent advances in transition metal-catalyzed C(sp^2)−H nitration. *Org. Biomol. Chem.* **2019**, *17*, 1351−1361. (c) Patel, S. S.; Patel, D. B.; Patel, H. D. Synthetic Protocols for Aromatic Nitration: A Review. *ChemistrySelect* **2021**, *6*, 1337−1356. (d) Qian, Y.-E.; Zheng, L.; Xiang, H.-Y.; Yang, H. Recent progress in the nitration of arenes and alkenes. *Org. Biomol. Chem.* **2021**, *19*, 4835−4851. (e) Zheng, Y.; Hu, Q.-Q.; Huang, Q.; Xie, Y. Late-Stage C−H Nitration of Unactivated Arenes by $Fe(NO_3)_3{\cdot}9H_2O$ in Hexafluoroisopropanol. *Org. Lett.* **2024**, *26*, 3316−3320.
(8) (a) Yan, G.; Borah, A. J.; Wang, L. Recent advances in the synthesis of nitroolefin compounds. *Org. Biomol. Chem.* **2014**, *12*, 6049−6058. (b) Bozorov, K.; Zhao, J.-Y.; Aisa, H. A. Recent advances in *ipso*-nitration reactions. *ARKIVOC: Online Journal of Organic Chemistry* **2017**, *2017*, 41.
(9) (a) Miyaura, N.; Suzuki, A. Palladium-catalyzed cross-coupling reactions of organoboron compounds. *Chem. Rev.* **1995**, *95*, 2457−2483. (b) Hall, D. G. *Boronic Acids: Preparation, Applications in Organic Synthesis and Medicine*; John Wiley & Sons, 2006. (c) Fyfe, J. W.; Watson, A. J. Recent developments in organoboron chemistry: old dogs, new tricks. *Chem.* **2017**, *3*, 31−55. (d) Zhou, Y.; Akkarasereenon, K.; Liu, L.; Lin, R.; Song, L.; Tong, R. Ecofriendly Protocol for *ipso*-Bromination of Arylboronic Acids. *Org. Lett.* **2024**, *26*, 5151−5156.
(10) (a) Salzbrunn, S.; Simon, J.; Prakash, G. K. S.; Petasis, N. A.; Olah, G. A. Regioselective Nitration of Arylboronic Acids. *Synlett* **2000**, *2000*, 1485−1487. (b) Prakash, G. K. S.; Panja, C.; Mathew, T.; Surampudi, V.; Petasis, N. A.; Olah, G. A. *ipso*-Nitration of Arylboronic Acids with Chlorotrimethylsilane−Nitrate Salts. *Org. Lett.* **2004**, *6*, 2205−2207. (c) Shen, G.; Zhao, L.; Liu, W.; Huang, X.; Song, H.; Zhang, T. Convenient, metal-free ipso-nitration of arylboronic acids using nitric acid and trifluoroacetic acid. *Synth. Commun.* **2017**, *47*, 10−14. (d) Zhang, K.; Budinská, A.; Passera, A.; Katayev, D. *N*-Nitroheterocycles: Bench-Stable Organic Reagents for Catalytic *Ipso*-Nitration of Aryl- and Heteroarylboronic Acids. *Org. Lett.* **2020**, *22*, 2714−2719. (e) Wu, X.-F.; Schranck, J.; Neumann, H.; Beller, M. Convenient and mild synthesis of nitroarenes by metal-free nitration of arylboronic acids. *Chem. Commun.* **2011**, *47*, 12462−12463. (f) Chatterjee, N.; Bhatt, D.; Goswami, A. A novel transition metal free [bis-(trifluoroacetoxy)iodo]benzene (PIFA) mediated oxidative *ipso* nitration of organoboronic acids. *Org. Biomol. Chem.* **2015**, *13*, 4828−4832. (g) Zarei, M.; Noroozizadeh, E.; Moosavi-Zare, A. R.; Zolfigol, M. A. Synthesis of Nitroolefins and Nitroarenes under Mild Conditions. *J. Org. Chem.* **2018**, *83*, 3645−3650. (h) Manna, S.; Maity, S.; Rana, S.; Agasti, S.; Maiti, D. *ipso*-Nitration of Arylboronic Acids with Bismuth Nitrate and Perdisulfate. *Org. Lett.* **2012**, *14*, 1736−1739. (i) Jiang, M.; Yang, H.; Li, Y.; Jia, Z.; Fu, H. Efficient *ipso*-nitration of arylboronic acids with iron nitrate as the nitro source. *RSC Adv.* **2013**, *3*, 25602−25604. (j) Murray, J. I.; Silva Elipe, M. V.; Baucom, K. D.; Brown, D. B.; Quasdorf, K.; Caille, S. *Ipso* Nitration of Aryl Boronic Acids Using Fuming Nitric Acid. *J. Org. Chem.* **2022**, *87*, 1977−1985.
(11) (a) Stephenson, C. R.; Yoon, T. P.; MacMillan, D. W. *Visible Light Photocatalysis in Organic Chemistry*; John Wiley & Sons, 2018. (b) Skubi, K. L.; Blum, T. R.; Yoon, T. P. Dual Catalysis Strategies in Photochemical Synthesis. *Chem. Rev.* **2016**, *116*, 10035−10074. (c) Romero, N. A.; Nicewicz, D. A. Organic Photoredox Catalysis. *Chem. Rev.* **2016**, *116*, 10075−10166. (d) Xuan, J.; Xiao, W.-J. Visible-Light Photoredox Catalysis. *Angew. Chem., Int. Ed.* **2012**, *51*, 6828−6838. (e) Studer, A.; Curran, D. P. Catalysis of Radical Reactions: A Radical Chemistry Perspective. *Angew. Chem., Int. Ed.* **2016**, *55*, 58−102. (f) Marzo, L.; Pagire, S. K.; Reiser, O.; König, B. Visible-Light Photocatalysis: Does It Make a Difference in Organic Synthesis? *Angew. Chem., Int. Ed.* **2018**, *57*, 10034−10072.
(12) (a) Wenger, O. S. Photoactive Complexes with Earth-Abundant Metals. *J. Am. Chem. Soc.* **2018**, *140*, 13522−13533. (b) Abderrazak, Y.; Bhattacharyya, A.; Reiser, O. Visible-Light-Induced Homolysis of Earth-Abundant Metal-Substrate Complexes: A Complementary Activation Strategy in Photoredox Catalysis. *Angew. Chem., Int. Ed.* **2021**, *60*, 21100−21115.
(13) (a) Shields, B. J.; Doyle, A. G. Direct C(sp^3)−H Cross Coupling Enabled by Catalytic Generation of Chlorine Radicals. *J. Am. Chem. Soc.* **2016**, *138*, 12719−12722. (b) Heitz, D. R.; Tellis, J. C.; Molander, G. A. Photochemical Nickel-Catalyzed C−H Arylation: Synthetic Scope and Mechanistic Investigations. *J. Am. Chem. Soc.* **2016**, *138*, 12715−12718. (c) Hu, A.; Guo, J.-J.; Pan, H.; Zuo, Z. Selective functionalization of methane, ethane, and higher alkanes by cerium photocatalysis. *Science* **2018**, *361*, 668−672. (d) Wen, L.; Ding, J.; Duan, L.; Wang, S.; An, Q.; Wang, H.; Zuo, Z. Multiplicative enhancement of stereoenrichment by a single catalyst for deracemization of alcohols. *Science* **2023**, *382*, 458−464. (e) Campbell, B. M.; Gordon, J. B.; Raguram, E. R.; Gonzalez, M. I.; Reynolds, K. G.; Nava, M.; Nocera, D. G. Electrophotocatalytic perfluoroalkylation by LMCT excitation of Ag (II) perfluoroalkyl carboxylates. *Science* **2024**, *383*, 279−284. (f) Treacy, S. M.; Rovis, T. Copper catalyzed C(sp^3)−H bond alkylation via photoinduced ligand-to-metal charge transfer. *J. Am. Chem. Soc.* **2021**, *143*, 2729−2735. (g) Sang, R.; Han, W.; Zhang, H.; Saunders, C. M.; Noble, A.; Aggarwal, V. K. Copper-mediated dehydrogenative C(sp^3)−H borylation of alkanes. *J. Am. Chem. Soc.* **2023**, *145*, 15207−15217. (h) Wang, M.; Huang, Y.; Hu, P. Terminal C(sp^3)−H borylation through intermolecular radical sampling. *Science* **2024**, *383*, 537−544. (i) Jin, Y.; Zhang, Q.; Wang, L.; Wang, X.; Meng, C.; Duan, C. Convenient C(sp^3)−H bond functionalisation of light alkanes and other compounds by iron photocatalysis. *Green Chem.* **2021**, *23*, 6984−6989. (j) Jin, Y.; Wang, L.; Zhang, Q.; Zhang, Y.; Liao, Q.; Duan, C. Photo-induced direct alkynylation of methane and other light alkanes by iron catalysis. *Green Chem.* **2021**, *23*, 9406−9411. (k) Zhang, Q.; Liu, S.; Lei, J.; Zhang, Y.; Meng, C.; Duan, C.; Jin, Y. Iron-Catalyzed Photoredox Functionalization of Methane and Heavier Gaseous Alkanes: Scope, Kinetics, and Computational Studies. *Org. Lett.* **2022**, *24*, 1901−1906. (l) Zhang, Y.; Fu, D.; Chen, Z.; Cui, R.; He, W.; Wang, H.; Chen, J.; Chen, Y.; Li, S.-J.; Lan, Y.; Duan, C.; Jin, Y. Bifunctional iron-catalyzed alkyne *Z*-selective hydroalkylation and tandem *Z*-*E* inversion via radical molding and flipping. *Nat. Commun.* **2024**, *15*, 8619. (m) Xu, P.; López-Rojas, P.; Ritter, T. Radical decarboxylative carbometalation of benzoic acids: a solution to aromatic decarboxylative fluorination. *J. Am. Chem. Soc.* **2021**, *143*, 5349−5354. (n) Chinchole, A.; Henriquez, M. A.; Cortes-Arriagada, D.; Cabrera, A. R.; Reiser, O. Iron (III)-light-induced homolysis: A dual photocatalytic approach for the hydroacylation of alkenes using acyl radicals via direct HAT from aldehydes. *ACS Catal.* **2022**, *12*, 13549−13554. (o) Lutovsky, G. A.; Gockel, S. N.; Bundesmann, M. W.; Bagley, S. W.; Yoon, T. P. Iron-mediated modular decarboxylative cross-nucleophile coupling. *Chem.* **2023**, *9*, 1610−1621. (p) Tu, J.-L.; Hu, A.-M.; Guo, L.; Xia, W. Iron-Catalyzed C(Sp^3)−H Borylation, Thiolation, and Sulfinylation Enabled by Photoinduced Ligand-to-Metal Charge Transfer. *J. Am. Chem. Soc.* **2023**, *145*, 7600−7611. (q) Zhang, Z.; Li, X.; Zhou, D.; Ding, S.; Wang, M.; Zeng, R. Controllable C−H Alkylation of Polyethers via Iron Photocatalysis. *J. Am. Chem. Soc.* **2023**, *145*, 7612−7620. (r) Yuan, X.-Y.; Wang, C.-C.; Yu, B. Recent advances in $FeCl_3$-photocatalyzed organic reactions via hydrogen-atom transfer. *Chin. Chem. Lett.* **2024**, *35*, 109517. (s) He, Y.; Tian, C.; An, G.; Li, G. β-C(sp^3)−H chlorination of amide derivatives via photoinduced copper charge transfer catalysis. *Chin. Chem. Lett.* **2024**, *35*, 108546. (t) Guo, J.-J.; Hu, A.; Chen, Y.; Sun, J.; Tang, H.; Zuo, Z. Photocatalytic C−C Bond Cleavage and Amination of Cycloalkanols by Cerium(III) Chloride Complex. *Angew. Chem., Int. Ed.* **2016**, *55*, 15319−15322. (u) Hu, A.; Guo, J.-J.; Pan, H.; Tang, H.; Gao, Z.; Zuo, Z. δ-Selective Functionalization of Alkanols Enabled by Visible-Light-Induced Ligand-to-Metal Charge Transfer. *J. Am.*

https://doi.org/10.1021/acscatal.4c07252
ACS Catal. 2025, 15, 3306−3313

Chem. Soc. **2018**, *140*, 1612−1616. (v) Chang, L.; An, Q.; Duan, L.; Feng, K.; Zuo, Z. Alkoxy Radicals See the Light: New Paradigms of Photochemical Synthesis. *Chem. Rev.* **2022**, *122*, 2429−2486. (w) An, Q.; Xing, Y.-Y.; Pu, R.; Jia, M.; Chen, Y.; Hu, A.; Zhang, S.-Q.; Yu, N.; Du, J.; Zhang, Y.; Chen, J.; Liu, W.; Hong, X.; Zuo, Z. Identification of Alkoxy Radicals as Hydrogen Atom Transfer Agents in Ce-Catalyzed C−H Functionalization. *J. Am. Chem. Soc.* **2023**, *145*, 359−376. (x) An, Q.; Chang, L.; Pan, H.; Zuo, Z. Ligand-to-Metal Charge Transfer (LMCT) Catalysis: Harnessing Simple Cerium Catalysts for Selective Functionalization of Inert C−H and C−C Bonds. *Acc. Chem. Res.* **2024**, *57*, 2915−2927. (y) Chang, L.; Wang, S.; An, Q.; Liu, L.; Wang, H.; Li, Y.; Feng, K.; Zuo, Z. Resurgence and advancement of photochemical hydrogen atom transfer processes in selective alkane functionalizations. *Chem. Sci.* **2023**, *14*, 6841−6859. (z) Pan, H.; An, Q.; Mai, B. K.; Chen, Y.; Liu, P.; Zuo, Z. Iron-Catalyzed Aerobic Carbonylation of Methane via Ligand-to-Metal Charge Transfer Excitation. *J. Am. Chem. Soc.* **2025**, *147*, 1440−1447.

(14) Liu, S.; Gan, Z.; Jiang, M.; Liao, Q.; Lu, Y.; Wang, H.; Xue, Z.; Chen, Z.; Zhang, Y.; Yang, X.; Duan, C.; Jin, Y. Selective Arene Photonitration via Iron-Complex β-Homolysis. *JACS Au* **2024**, *4*, 4899−4909.

(15) Moulin, E.; Armao, J. J. I. V.; Giuseppone, N. Triarylamine-Based Supramolecular Polymers: Structures, Dynamics, and Functions. *Acc. Chem. Res.* **2019**, *52*, 975−983.

(16) Buettner, G. R. Spin Trapping: ESR parameters of spin adducts 1474 1528V. *Free Radical Biol. Med.* **1987**, *3*, 259−303.

(17) Li, M.; Li, H.; Ling, C.; Shang, H.; Wang, H.; Zhao, S.; Liang, C.; Mao, C.; Guo, F.; Zhou, B.; Ai, Z.; Zhang, L. Highly selective synthesis of surface Fe^{IV}═O with nanoscale zero-valent iron and chlorite for efficient oxygen transfer reactions. *Proc. Natl. Acad. Sci. U. S. A.* **2023**, *120*, No. e2304562120.

https://doi.org/10.1021/acscatal.4c07252
ACS Catal. 2025, 15, 3306−3313